https://doi.org/10.5194/essd-2026-463
Preprint. Discussion started: 25 June 2026

Open Access Earth System Science Data Discussions

Coastal Atmosphere & Sea Time Series (CoASTS) and Bio-Optical mapping of Marine optical Properties (BiOMaP): the hyperspectral absorption coefficients by optically significant constituents.

Jean-François Berthon[1] and Giuseppe Zibordi[2,3]

[1]*Joint Research Centre of the European Commission, Ispra, Italy*
[2]*National Aeronautics and Space Administration, Goddard Space Flight Center, MD USA*
[3]Southeastern Universities Research Association, Washington. DC 20005 USA

Correspondence to: Jean-François Berthon (jean-francois.berthon@ec.europa.eu)

https://doi.org/10.5194/essd-2026-463
Preprint. Discussion started: 25 June 2026

Open Access Earth System Science Data Discussions

ABSTRACT

The *Coastal Atmosphere & Sea Time Series* (CoASTS) and the *Bio-Optical mapping of Marine optical Properties* (BiOMaP) programs were conceived and implemented to assist ocean color applications with field measurements of apparent and inherent optical properties, and concentration of optically significant water constituents. The CoASTS program led to the creation of time-series of bio-optical measurements at the Acqua Alta Oceanographic Tower (AAOT) site the northern Adriatic Sea continued from 1995 up to 2016. The BiOMaP program supported the collection of equivalent bio-optical measurements across European Seas from 2000 up to 2022. This work focusses on CoASTS and BiOMaP hyperspectral absorption coefficients of optically significant constituents as determined applying standardized instruments, community measurement methods, extended quality control schemes and consolidated processing codes. The work, which complements a previous one by Zibordi and Berthon (2024) centred on multi-spectral data, presents the CoASTS and BiOMaP hyperspectral absorption coefficients of pigmented and non-pigmented particles in the 400-750 nm, and of colored dissolved organic matter in the 350-680 nm interval, both with a 3 nm spectral resolution at 2 nm increment.

https://doi.org/10.5194/essd-2026-463
Preprint. Discussion started: 25 June 2026

Open Access Earth System Science Data Discussions

1. Introduction

Over a period exceeding two decades, the *Coastal Atmosphere & Sea Time Series* (CoASTS) and the *Bio-Optical mapping of Marine optical Properties* (BiOMaP) field programs led to the collection of *in situ* bio-optical measurements to support ocean color applications. The CoASTS and BiOMaP programs, established by the Marine Optical Laboratory of the Joint Research Centre (JRC) in collaboration with several European research institutions, ensured: *i.* time-series measurements at the Acqua Alta Oceanographic Tower (AAOT) site in the northern Adriatic Sea characterized by moderately optically complex waters (Berthon et al. 2002; Zibordi et al. 2002); and *ii*. geographically distributed ship-based measurements across major European Seas exhibiting a variety of water types (Berthon et al. 2008, Zibordi et al. 2011).

This work presents the CoAST-BiOMaP data set of hyperspectral absorption coefficients determined applying spectrophotometric methods to field marine water samples. Opposite to the multi-spectral absorption coefficients accompanying a previous dataset of radiometric data products (Zibordi and Berthon 2024), this complementary dataset comprises absorption coefficients exhibiting 3 nm spectral resolutions at 2 nm increment for pigmented and non-pigmented particles in the 400-750 nm, and for colored dissolved organic matter in the 350-680 nm interval. This unique dataset is expected to fulfil application needs for bio-optical investigations supporting the new generation of hyperspectral satellite ocean color sensors (e.g., Werdell et al. 2026).

2. The CoASTS and BiOMaP paired measurement programs

CoASTS time-series started in 1995 with monthly sampling frequency, later reduced to bi-monthly (or less) up to the end of the program in 2016. CoASTS measurements comprised in-water optical and hydrographic profiles, water samples from near surface, 8 m and 14 m depth, meteorological data, and cloud cover and sea state observations. Bio-optical characteristics (Berthon et al. 2002) are representative of marine regions with optical properties generally determined by moderate concentrations of sediments and colored dissolved organic matter (CDOM) and or occasionally by phytoplankton and its degradation components, *i.e.*, Case-1 waters (IOCCG 2000).

BiOMaP ship-based campaigns were performed from 2000 up to 2022 in the major European seas (see Berthon et al. 2008): the Baltic Sea exhibiting waters characterized by a high concentration of CDOM; the Adriatic Sea, Black Sea, Iberian Shelf, Greenland Sea, Ligurian Sea, and North Sea, exhibiting diverse concentrations of CDOM and suspended particulate matter (*SPM*); and finally the Eastern and Western Mediterranean Seas with oligotrophic and mesotrophic Case-1 waters. BiOMaP stations included the same measurements and observations as CoASTS, but water sampling was limited to the near-surface layer.

Data consistency across the two programs was ensured through the application of standardized instruments, community measurement methods, extended quality control schemes and consolidated processing codes.

Out of the 176 CoASTS field campaigns, only the 125 performed from December 1998 and leading to a total of 637 stations are included in the current dataset. This choice has been suggested by the objective to populate the dataset with those data fulfilling standardized methods and data reduction processes. Conversely, all the 36 BiOMaP campaigns for a total of 1915 stations, are included in the dataset.

Details on the CoASTS and BiOMaP measurement stations are summarized in Tables 1 and 2, respectively, reproduced from Zibordi and Berthon (2024). The reader is also addressed to the

https://doi.org/10.5194/essd-2026-463
Preprint. Discussion started: 25 June 2026

same publication for figures presenting the temporal and geographic distribution of the CoASTS and BiOMaP stations, respectively.

Table 1. CoASTS campaign identifiers, marine region, year, number of stations, research platform, collaborating institution (after Zibordi and Berthon 2024).

Campaign ID	Location	Year	Stations #	Research platform	Collaborating Institution
V03-V99	Northern Adriatic Sea (AAOT)	1998-2011	481	*Acqua Alta Oceanog. Tower (AAOT)*	Italian National Research Council (IT)
W01-W28	Northern Adriatic Sea (AAOT)	2011-2016	136	*Acqua Alta Oceanog. Tower (AAOT)*	Italian National Research Council (IT)

Table 2. BiOMaP campaign identifiers, marine regions, year, number of stations, research vessels, collaborating institutions (after Zibordi and Berthon 2024).

Campaign ID	Region	Year	Stations #	Research vessel	Collaborating Institution
A01	Adriatic Sea (ADRS)	2000	55	*R/V Friuli-Venezia Giulia (FVG)*	University of Trieste (IT)
A02	Adriatic Sea (ADRS)	2014	66	*R/V Minerva-1*	Italian National Research Council (IT)
B01	Baltic Sea (BLTS)	2004	52	*R/V Oceania*	Institute of Oceanology (PL)
B02	Baltic Sea (BLTS)	2004	52	*R/V Oceania*	Institute of Oceanology (PL)
B03	Baltic Sea (BLTS)	2005	63	*R/V Oceania*	Institute of Oceanology (PL)
B04	Baltic Sea (BLTS)	2006	23	*R/V Aranda*	Institute of Marine Research (FI)
B05	Baltic Sea (BLTS)	2007	38	*R/V Aranda*	Institute of Marine Research (FI)
B06	Baltic Sea (BLTS)	2008	47	*R/V Aranda*	Institute of Marine Research (FI)
E01	Eastern Med. Sea (EMED)	2006	62	*R/V Urania*	Italian National Research Council (IT)
E02	Eastern Med. Sea (EMED)	2007	69	*R/V Urania*	Italian National Research Council (IT)
E03	Eastern Med. Sea (EMED)	2017	51	*R/V Minerva-1*	Italian National Research Council (IT)
E04	Eastern Med. Sea (EMED)	2022	31	*R/V Philia*	Hellenic Centre for Marine Research (GR)
I01	Iberian Shelf (IBSH)	2011	68	*NRP Almirante Gago Coutinho*	Portuguese Hydrographic Institute (PT)
I02	Iberian Shelf (IBSH)	2017	62	*NRP Almirante Gago Coutinho*	Portuguese Hydrographic Institute (PT)
K01	Black Sea (BLKS)	2006	93	*R/V Akademik*	Institute of Oceanology (BG)
K02	Black Sea (BLKS)	2009	73	*R/V Akademik*	Institute of Oceanology (BG)
K03	Black Sea (BLKS)	2009	40	*R/V Akademik*	Institute of Oceanology (BG)

https://doi.org/10.5194/essd-2026-463
Preprint. Discussion started: 25 June 2026

K04	Black Sea (BLKS)	2011	38	*R/V Mare Nigrum*	National Institute of Marine Geology and Geoecology (RO)
K05	Black Sea (BLKS)	2011	24	*R/V Akademik*	Institute of Oceanology (BG)
K06	Black Sea (BLKS)	2011	59	*R/V Akademik*	Institute of Oceanology (BG)
K07	Black Sea (BLKS)	2012	93	*R/V Akademik*	Institute of Oceanology (BG)
K08	Black Sea (BLKS)	2012	14	*R/V Akademik*	Institute of Oceanology (BG)
K09	Black Sea (BLKS)	2016	54	*R/V Akademik*	Institute of Oceanology (BG)
K10	Black Sea (BLKS)	2016	83	*R/V Akademik*	Institute of Oceanology (BG)
K11	Black Sea (BLKS)	2019	80	*R/V Akademik*	Institute of Oceanology (BG)
K12	Black Sea (BLKS)	2019	44	*R/V Akademik*	Institute of Oceanology (BG)
L01	Ligurian Sea (LIGS)	2008	41	*R/V Alliance*	Undersea Research Center (NATO)
L02	Ligurian Sea (LIGS)	2009	63	*R/V Alliance*	Undersea Research Center (NATO)
L04	Ligurian Sea (LIGS)	2013	25	*R/V Alliance*	Undersea Research Center (NATO)
N01	English Channel & North Sea (NORS)	2004	55	*R/V Côtes de la Manche*	Université du Littoral Côte d'Opale (FR)
N02	North Sea (NORS)	2015	52	*R/V Belgica*	Royal Belgian Institute of Natural Sciences (BE)
O01	Western Med. Sea (WMED)	2012	73	*R/V Urania*	Italian National Research Council (IT)
O02	Western Med. Sea (WMED)	2014	64	*R/V Urania*	Italian National Research Council (IT)
O03	Western Med. Sea (WMED)	2021	53	*R/V Garcia del Cid*	Institute of Marine Science (ES)
P01	Greenland Sea (GRLS)	2018	15	*R/V Alliance*	Undersea Research Center (NATO)
P03	Greenland Sea[1] (GRLS)	2021	40	*R/V Alliance*	Italian Hydrographic Institute (IT)

[1] It includes stations from the Norwegian Sea.

https://doi.org/10.5194/essd-2026-463
Preprint. Discussion started: 25 June 2026

Open Access Earth System Science Data Discussions

3. Details on the absorption measurement methods

CoASTS and BiOMaP laboratory measurements ensured the determination of the following spectral absorption coefficients from discrete water samples collected at approximately 1 m depth:

- a_{ph} and a_{dt} for pigmented and for non-pigmented particles, respectively;
- a_{ys} for CDOM.

Details on the applied measurement methods are given in the following subsections.

3.1 Absorption coefficient of particulate matter

The Transmission-Reflection (*T*-*R*) method by Tassan and Ferrari (1995, 2002), which was shown appropriate for any particle type including highly absorbing sediments or highly back-scattering mineral particles, was applied to determine the absorption coefficients by water particles collected on glass fiber filter The *T*-*R* method combines light transmittance (*T*) and light reflectance (*R*) measurements carried out using an integrating sphere combined with a dual-beam spectrophotometer. The method enables the measurement of both forward-scattered (*T*-mode) and backward-scattered (*R*-mode) light resulting from the interaction with the particles on the filter. Data reduction is supported by a theoretical model that minimizes the impact of differences in the light backscattered by the particles. The method was initially applied using a Perkin Elmer Lambda-19 spectrometer, replaced by a Lambda-950 from 2004 onward.

Whatman GF/F glass fibre filters with 0.7 µm pore size and 25 mm diameter were used to collect water particles from known water volumes. Following Tassan and Ferrari (2002), the total absorption coefficient $a_p(\lambda)$ of the equivalent particle suspension was determined in the 400-750 nm spectral interval with 1 nm resolution from

$$a_p(\lambda) = 2.3\, A_s(\lambda)\, (F_a / V_w)^{-1} \quad (1)$$

where V_w, F_a and $A_s(\lambda)$ are the filtered water volume, the filter clearance area and the equivalent particle suspension absorbance obtained with the *T*-*R* method, respectively.

A solution of sodium hypochlorite (NaClO) was applied to the sample to discriminate the non-pigmented fraction $a_{dp}(\lambda)$ from the total $a_p(\lambda)$, which allowed to determine the pigmented fractions as $a_{ph}(\lambda) = a_p(\lambda) - a_{ph}(\lambda)$.

The bleaching approach, which rapidly acts on pigment molecules and only slowly on detritus, is comprehensively discussed in Tassan and Ferrari (1995) and in Ferrari and Tassan (1999). Building on that approach, since 2003 a more controlled depigmentation methodology was implemented. This combines the chemical bleaching based on sodium hypochlorite solution with photo-bleaching, and additionally applies a real-time control of the depigmentation process through the monitoring of the sample reflectance in the red spectral region (Zibordi and Sciuto 2022). Such a methodology accelerates the bleaching process and prevents successive measurement trials to achieve an optimal depigmentation of the particles on the filter. In fact, the original approach requires successive additions of oxidizing agent and rinsing of the filter to remove the oxidation products. These imply an incremental determination of the absorbance by bleached particles, but also an unavoidable perturbation of particles distribution on the filter. Definitively, the implementation of the improved methodology allowed for the standardization of the bleaching process and warranted a better accuracy and reproducibility of the derived absorption coefficients.

https://doi.org/10.5194/essd-2026-463
Preprint. Discussion started: 25 June 2026

Open Access Earth System Science Data Discussions

Final $a_{dt}(\lambda)$ and $a_{ph}(\lambda)$ data products were determined with 3 nm spectral resolution at 2 nm increment. The spectral averaging applied to the actual laboratory measurements performed with 1 nm resolution, makes the $a_{dt}(\lambda)$ and $a_{ph}(\lambda)$ final data products less dependent on measurement noise, still at the expense of a reduced spectral resolution.

Well appreciating any previous effort addressing the accuracy of the *T-R* method (*e.g.,* Tassan and Ferrari (1995) and Tassan et al. (2000)), uncertainties for $a_{ph}(\lambda)$ and $a_{dp}(\lambda)$ are not available. Because of this, results from the analysis of $a_p(\lambda)$ measurement precision by Zibordi et al. (2002) are further recalled. That specific investigation addressed the precision of $a_p(\lambda)$ determined with the *T-R* method through: *i*. $a_p(\lambda)$ from repeated measurements of the same sample and *ii*. $a_p(\lambda)$ from replicated measurements of independent samples, still obtained from the same water volume. Results are summarized in Table 3 at the 443, 555 and 665 nm center-wavelengths through mean absolute percent differences (MAPD). Results show increasing MAPD values with wavelength. MADP for the absorption coefficients from repeated measurements of the same sample are mostly explained by: *i.* the sensitivity of the method, and *ii*. the lack of precision in re-positioning the filter in front of the aperture of the integrating sphere. The increased MADP of replicated measurements with respect to the repeated ones, are explained by: *i.* differences resulting from uneven distributions of particles on filters across replicates; *ii*. inhomogeneity of particles spreading in the water volumes collected to produce the samples; *iii.* uncertainty in the determination of the water volume.

Table 3. Absolute mean percent differences (MAPD) ± their standard deviations for repeated and replicated measurements of a_p at 443, 555 and 665 nm. The values in parenthesis indicate the average of the a_p spectral values ± their standard deviation, in units of m^{-1}. N is the number of samples.

λ [nm]	443	555	665
MAPD for repeated a_p [%] N=21	2.9±2.3 (0.082±0.042)	7.4±6.0 (0.023±0.011)	7.2 ±5.8 (0.027±0.015)
MAPD for replicated a_p [%] N=21	8.9±5.9 (0.090±0.049)	9.8±7.0 (0.024±0.012)	10.7 ±7.6 (0.028±0.017)

3.2 Absorption coefficient by CDOM

A Perkin Elmer Lambda-12 dual-beam spectrometer, and a Lambda-35 from 2010 onward, were used to determine $a_{ys}(\lambda)$ applying the method by Ferrari et al. (1996). Field samples were obtained by filtering water on Millipore 0.22 µm pore size cellulose filters. To prevent bacteria growth, 1mL of a solution of 10 g L^{-1} of NaN_3 was added to a 100 mL sample.

Spectrometric measurements were performed in the 350-750 nm spectral interval with 1 nm resolution by placing a 10 cm quartz cuvette containing the sample in the optical path of the spectrometer beam and an identical cuvette containing milli-Q water in the optical path of the reference beam. Definitively, 10 cm path-lengths may decrease the accuracy of measurements performed on samples exhibiting low CDOM absorption. Still, the need for standardizing measurements across the CoASTS and BiOMaP measurement programs embracing diverse geographic regions was a priority.

https://doi.org/10.5194/essd-2026-463
Preprint. Discussion started: 25 June 2026

Open Access Earth System Science Data Discussions

With reference to Ferrari et al. (1996) the absorption coefficient $a_{ys}(\lambda)$ was computed from the absorbance $A_{ys}(\lambda)$ resulting from the difference between the sample and reference ones, as

$$a_{ys}(\lambda) = 2.3\, A_{ys}(\lambda)\, L_c^{-1} \quad (2)$$

where L_c is the pathlength of the cuvette.

Assuming that CDOM absorption is nil in the red, the final absorption coefficients were obtained by subtracting the mean of the $a_{ys}(\lambda_i)$ spectral values for any $\lambda_i \in$ 670-680 nm to the measured $a_{ys}(\lambda)$. Consistent with $a_{ph}(\lambda)$ and $a_{dt}(\lambda)$, also the final $a_{ys}(\lambda)$ values are made available with 3 nm spectral resolution at 2 nm increment, but restricted to the 350-680nm interval.

Comprehensive uncertainty analysis are also not available for $a_{ys}(\lambda)$. Because of this, results from $a_{ys}(\lambda)$ precision analysis from Zibordi et al. (2002) are summarized too in Table 4 at the center-wavelenghts 412, 443 and 555 nm. This specific investigation looked at measurement precision through: $a_{ys}(\lambda)$ from repeated measurements of the same sample and *ii*. $a_{ys}(\lambda)$ from replicated measurements of independent samples, still obtained from the same water volume. Similar to results obtained for $a_p(\lambda)$, MAPD determined for $a_{ys}(\lambda)$ exhibit values largely increasing with wavelength consistently with the exponential decrease of $a_{ys}(\lambda)$ toward the red. MADP from repeated measurements are largely due to the precision of the method. Unavoidable differences affecting sample replicates are responsible for the increase of MAPD of replicated measurements with respect to those of the repeated ones.

Table 4. Absolute MAPD ± their standard deviations, determined for repeated and replicated measurements of a_{ys} at 412, 443 and 555 nm. The values in parenthesis indicate the average of the a_{ys} spectral values ± their standard deviation, in units of m^{-1}. N is the number of samples.

λ [nm]	412	443	555
APD for repeated a_{ys} [%] N=21	10.1±7.3 (0.168±0.037)	12.4±8.4 (0.097±0.022)	24.2 ±19.8 (0.015±0.005)
APD for replicated a_{ys} [%] N=21	12.1±6.3 (0.175±0.038)	15.8±8.8 (0.103±0.026)	30.3 ±23.8 (0.018±0.005)

4. The CoASTS and BiOMaP dataset of hyperspectral absorption coefficients

CoASTS-BiOMaP hyperspectral data of absorption coefficients are accessible in tabular form at https://doi.org/10.1594/PANGAEA.XXXXXX.

Details on the quantities constituting the dataset are provided in Table 5. Nevertheless, the reader is addressed to Zibordi and Berthon (2024) for a comprehensive description of all the field and laboratory measurements complementing the hyperspectral absorption coefficients matter of this work. It is anticipated that the number of measurement stations included in the present dataset is slightly higher than the one constituting the multi-spectral dataset. This is explained by the quality control applied to hyperspectral data, fully independent of other measured quantities (see Zibordi and Berthon, 2024). Still some a_{ys} spectra were not included in the hyperspectral dataset because of unrealistically low values in the ultraviolet and blue spectral region.

https://doi.org/10.5194/essd-2026-463
Preprint. Discussion started: 25 June 2026

Open Access Earth System Science Data Discussions

Figures 1-3 display BioMaP and CoASTS $a_{ph}(\lambda)$, $a_{dt}(\lambda)$ and $a_{ys}(\lambda)$ spectra for the different marine regions. Some of these spectra refer to bio-optical cases typical of Eastern Mediterranean Sea (EMED) oligotrophic waters and Baltic Sea (BLTS) CDOM dominated waters. Between these two extremes, there are spectra from the North Sea (NORS), characterized by relatively high concentrations of non-organic particles, and from the Black Sea (BLKS) and northern Adriatic Sea (AAOT) exhibiting optical characteristics determined by variable concentrations of SPM and CDOM.

Table 5. Details on the quantities included in the CoASTS-BiOMaP hyperspectral dataset defined in agreement with the notations already used in Zibordi and Berthon (2024).

Symbol	***Description***	***Units***	***Details***
Station_ID	Station identifier	Code	*Gccssii*[(1)]
Date&Time	Date and time	GMT	*yyyy-mm-dd*T*hh:mm:ss*[(2)]
Lon	Longitude	Degrees	
Lat	Latitude	Degrees	
$a_{ph}(\lambda)$	Absorption coefficient by pigmented particles at 1 m depth	m^{-1}	3 nm spectral resolution at 2 nm increment in 400-750 nm interval
$a_{dt}(\lambda)$	Absorption coefficient by non-pigmented part. at 1 m depth	m^{-1}	3 nm spectral resolution at 2 nm increment in 400-750 nm interval
$a_{ys}(\lambda)$	Absorption coefficient by CDOM at 1 m depth	m^{-1}	3 nm spectral resolution at 2 nm increment in 350-680 nm interval

[1] *G* indicates the site or geographic region (V and W for AAOT, A for Adriatic Sea, B for Baltic Sea, E for Eastern Mediterranean Sea, K for Black Sea, L for Ligurian Sea, N for North Sea, O for Western Mediterranean Sea, I for Iberian Shelf, P for Greenland Sea), while *cc* indicates the campaign number for the specific region, *ss* the station number and *ii* the cast number.
[2] The letters *yyyy* indicate the year, *mm* the month, *dd* the day *hh,* the hours, *mm* the minutes and *ss* the seconds.

Figure 1 displays the a_{ph} spectra for the various marine regions. The increase in the mean values of $a_{ph}(\lambda)$ around 440 nm from approximately 0.01 m^{-1} for the Eastern Mediterranean Sea (EMED) waters to values approaching 0.2 m^{-1} for the Baltic Sea (BLTS) and North Sea (NORS) ones, is noteworthy. Some North Sea (NORS) spectra from samples collected off the Belgian coast exhibit values of a_{ph} higher at 400 nm than at 440 nm. This is explained by high concentrations of pheophytin leading to an increase of the absorption coefficient toward 400 nm (Zibordi and Berthon 2024). Finally, a few a_{ph} spectra were noted to exhibit unrealistic negative values beyond approximately 500 nm. This is explained by limits of the measurement methodology in the presence of a low concentration of particles largely associated with oligotrophic regions. These spectra were not excluded from the data set expecting their application can be still relevant if the absorption coefficients are corrected for their background in the near-infrared.

The $a_{dt}(\lambda)$ spectra displayed in Fig. 2 exhibit the expected exponential decay from 400 nm to 750 nm, even though sometimes affected by minor irregularities such as the shoulders around 480-490 nm, which indicate a potential uncomplete bleaching of accessory pigments. Mean values of a_{dt} at 400 nm consistently vary from approximately 0.01 m^{-1} for the Mediterranean Sea (either EMED and WMED) waters, exceed 0.06 m^{-1} for the Adriatic Sea (AAOT) ones, and

https://doi.org/10.5194/essd-2026-463
Preprint. Discussion started: 25 June 2026

Open Access Earth System Science Data Discussions

reach 0.11 m^{-1} for the Baltic Sea (BLTS). The residual values of $a_{dt}(\lambda)$ in the near-infrared reflect actual absorption by non-living particles.

Figure 3 displays the $a_{ys}(\lambda)$ spectra in the 350-680 nm spectral interval. The mean values of a_{ys} at 350 nm largely vary across marine regions. In agreement with the oligotrophic nature of the Eastern Mediterranean Sea (EMED) waters and the highly absorbing Baltic Sea (BLTS) ones, a minimum value of 0.13 m^{-1} is observed for the first while a maximum of 2.2 m^{-1} characterizes the second.

Of major interest are the slopes S_{dt} and S_{ys} defining the exponential decay of $a_{dt}(\lambda)$ and $a_{ys}(\lambda)$, for which the readers are addressed to Zibordi and Berthon (2024). Those authors determined the parameters defining the best exponential fit versus wavelength of $a_{dt}(\lambda)$ and $a_{ys}(\lambda)$ within the 412-665 nm spectral interval using

$$a_{dt}(\lambda) = A_{dt} \exp(-S_{dt}(\lambda - 412)) + B_{dt} \quad (3)$$

and

$$a_{ys}(\lambda) = A_{ys} \exp\left(-S_{ys}(\lambda - 412)\right) + B_{ys}, \quad (4)$$

where A_{dt} and A_{ys} indicate the absorption coefficients fitted at 412 nm, S_{dt} and S_{ys} the slope of the exponential function, and, B_{dt} and B_{ys} account for the background.

With reference to Zibordi and Berthon (2024), the slopes S_{dt} exhibit mean values varying from 0.009 nm^{-1} for the Eastern Mediterranean Sea (EMED) up to 0.013 for the North Sea (NORS). Similarly, the slopes S_{ys} show mean values ranging from 0.012 nm^{-1} for the Eastern Mediterranean Sea (EMED) up to 0.019 nm^{-1} for the Baltic Sea (BLTS).

Ternary plots of a_{ys}, a_{dt} and a_{ph} at 442 nm as a percent of the total absorption (*i.e.*, $a_{ys}(442)+a_{dt}(442)+a_{ph}(442)$) are presented in Fig. 4. Consistent with the equivalent plots presented in Zibordi and Berthon (2024), very few cases (most refer to the Black Sea for values greater than 60%) suggest dominance of absorption by particles with a_{ph} and a_{dt} values clustering near the upper and lower right vertices, respectively. Indeed, most of the cases show predominance of absorption by CDOM with a_{ys} values clustered nearby the lower left vertex. While this is naturally expected for the Black Sea (BLKS) optically complex waters and for all the Baltic Sea (BLTS) highly absorbing ones, peculiar is the pronounced clustering observed for the Eastern Mediterranean Sea (EMED) oligotrophic waters, and also for some geographic areas of the Western Mediterranean Sea (WMED) oligotrophic/mesotrophic ones. This outcome for either EMED and WMED waters, conflicts with the Case-1 water classification (IOCCG 2000). Still, equivalent findings were reached by Pérez et al. (2016), further confirming the presence of a significant CDOM background in the Mediterranean Sea waters

Minor differences between Fig. 4 and the equivalent one published in Zibordi and Berthon (2024) are explained by the diverse number of spectra (see § 4).

As an applicative example, scatter plots of $a_{ph}(442)$ versus $a_{ph}(676)$ in m^{-1} are displayed in Fig. 5 to investigate the impact of regional pigments. As expected, data show decreasing values of the average $a_{ph}(442)/a_{ph}(676)$ ratio from oligotrophic (*i.e.,* EMED and WMED) to more eutrophic waters (*i.e.,* NORS and BLTS), with the exception of the high value characterizing the Black Sea (BKLS). This suggests a higher mean cell size (and consequently an increased packaging effect) in conjunction with a lower proportion of photoprotective pigments in eutrophic environments, which lead to a lower ratio with respect to oligotrophic environments.

https://doi.org/10.5194/essd-2026-463
Preprint. Discussion started: 25 June 2026

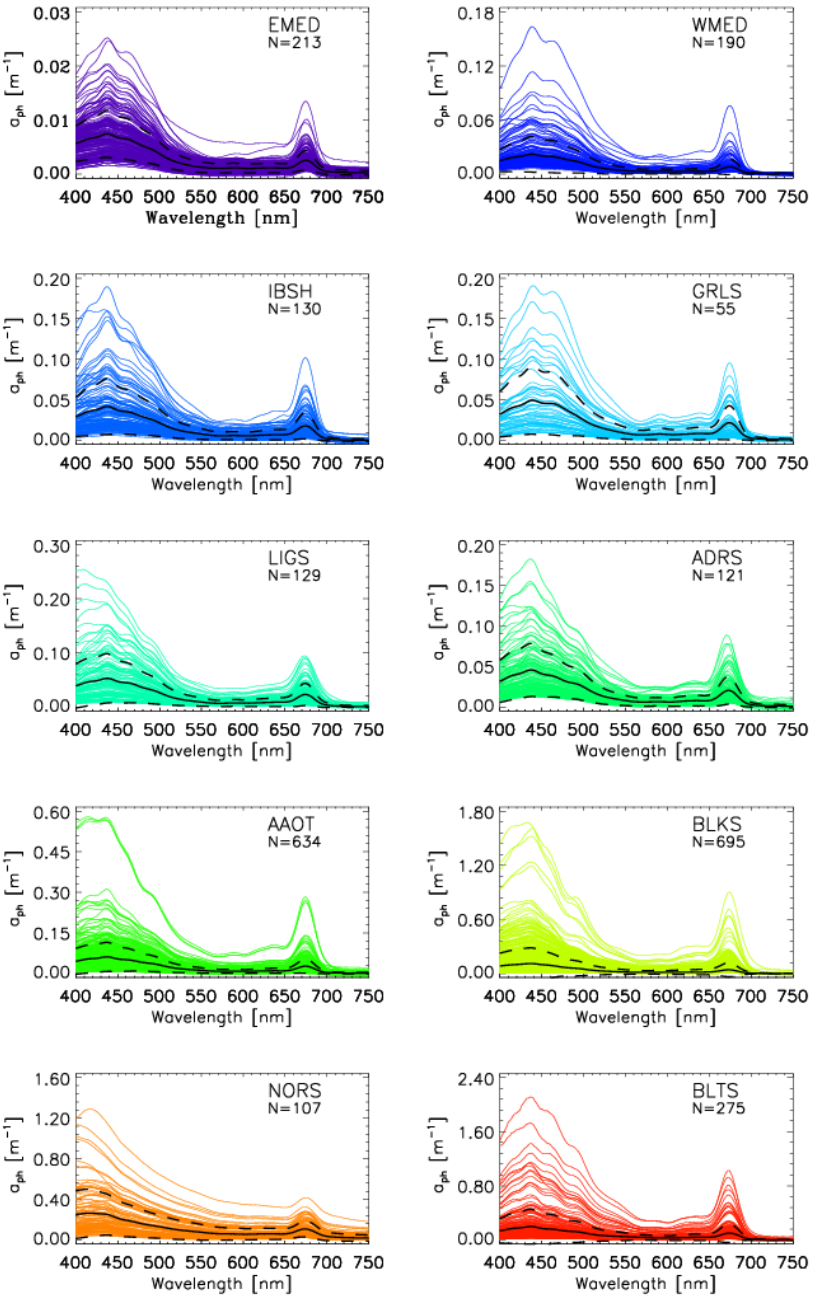

Figure 1. Spectra of $a_{ph}(\lambda)$ for the various marine regions. N is the number of spectra. The continuous thick black lines indicate mean values while the dashed lines indicate ± 1 standard deviation.

https://doi.org/10.5194/essd-2026-463
Preprint. Discussion started: 25 June 2026

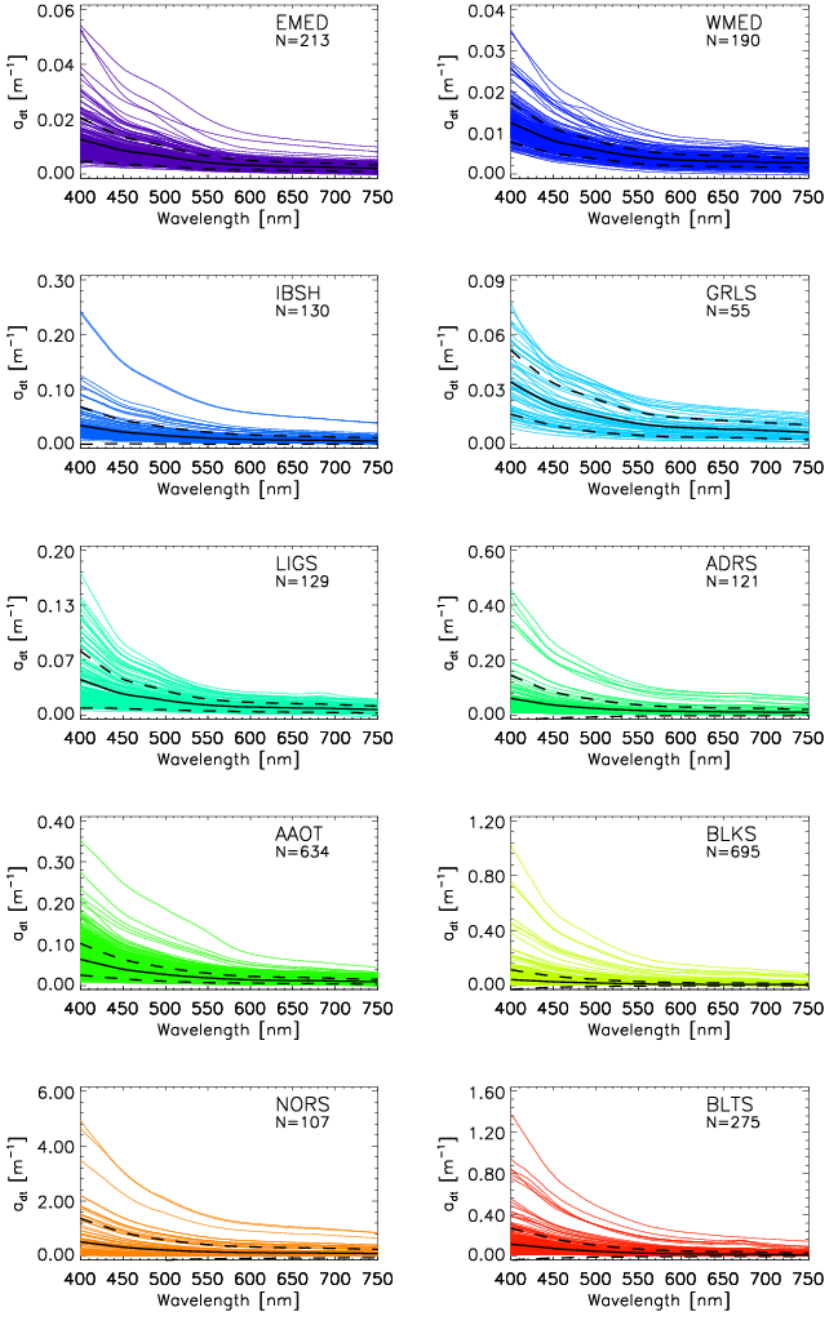

Figure 2. Spectra of $a_{dt}(\lambda)$ for the various marine regions. N is the number of spectra. The continuous thick black lines indicate mean values while the dashed lines indicate ± 1 standard deviation.

https://doi.org/10.5194/essd-2026-463
Preprint. Discussion started: 25 June 2026

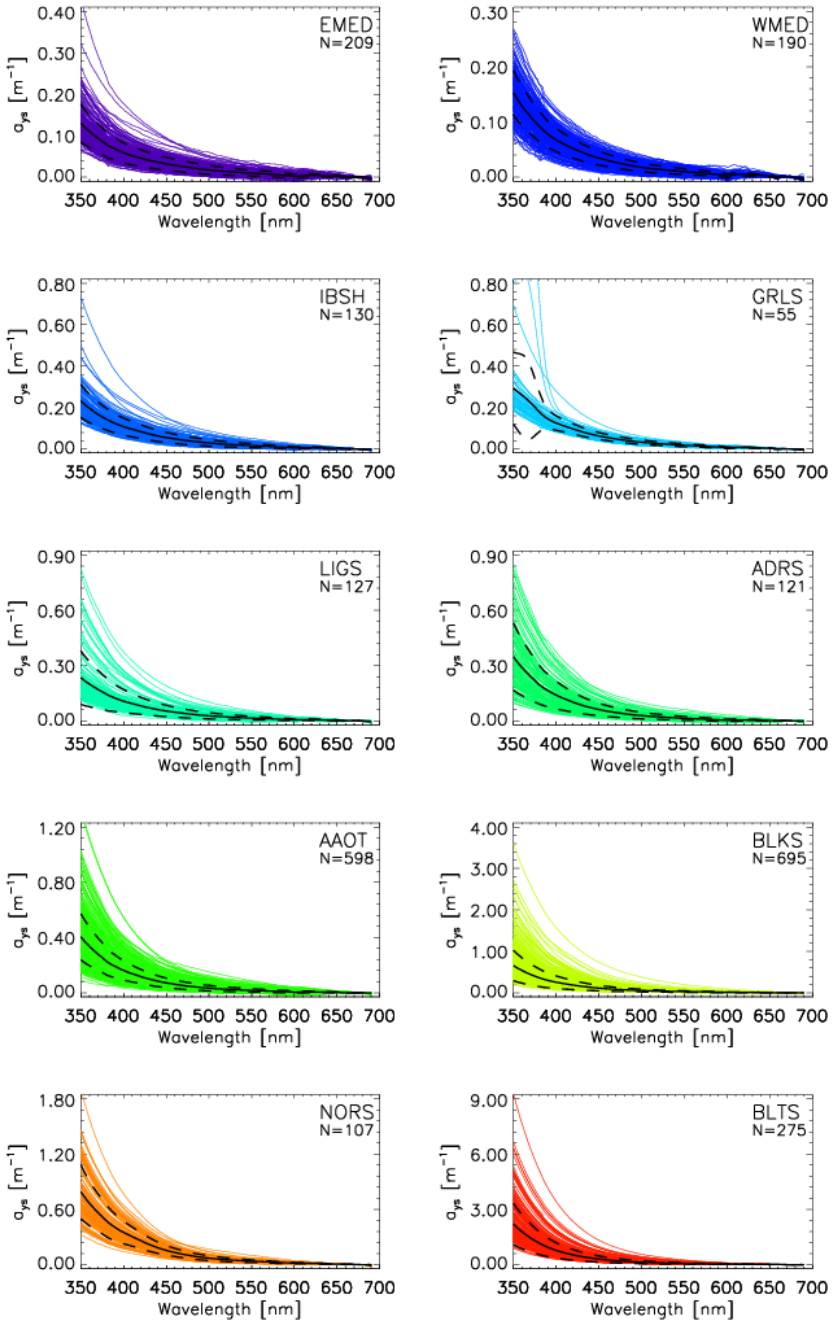

Figure 3. Spectra of $a_{ys}(\lambda)$ for the various marine regions. N is the number of spectra. The continuous black lines indicate mean values while the dashed lines indicate ± 1 standard deviation.

https://doi.org/10.5194/essd-2026-463
Preprint. Discussion started: 25 June 2026

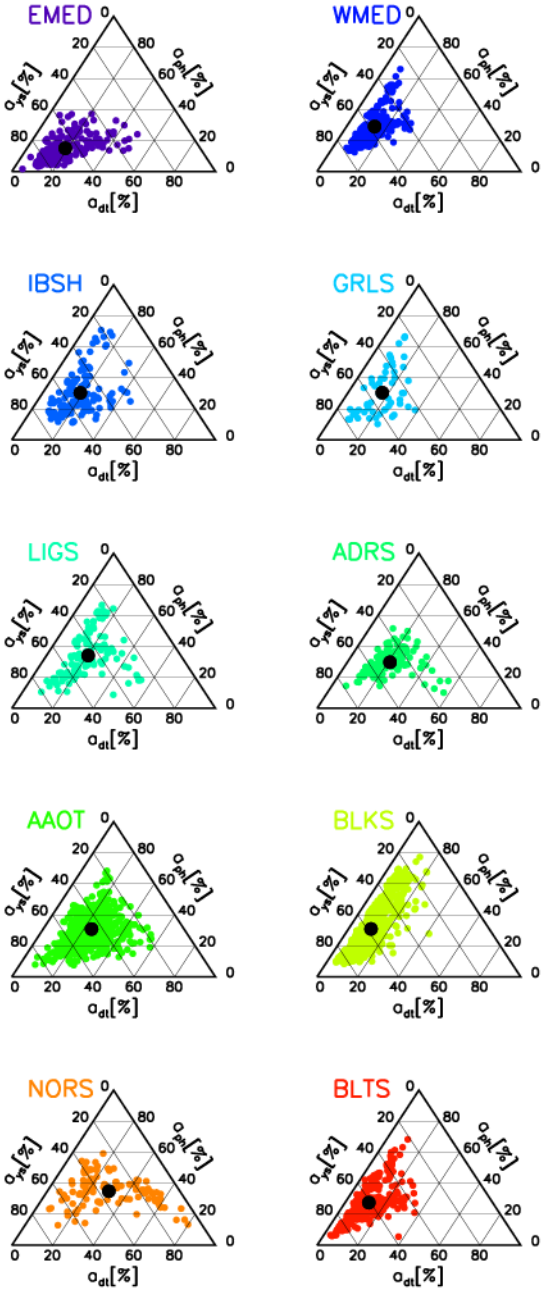

Figure 4. Ternary plots of the absorption coefficients a_{ys}, a_{dt} and a_{ph} expressed in percent of the total (except sea water) absorption (*i.e.*, with respect to $a_{ys}+a_{dt}+a_{ph}$) at the 442 nm center-wavelength. The filled black circles indicates the mean of the plotted values.

https://doi.org/10.5194/essd-2026-463
Preprint. Discussion started: 25 June 2026

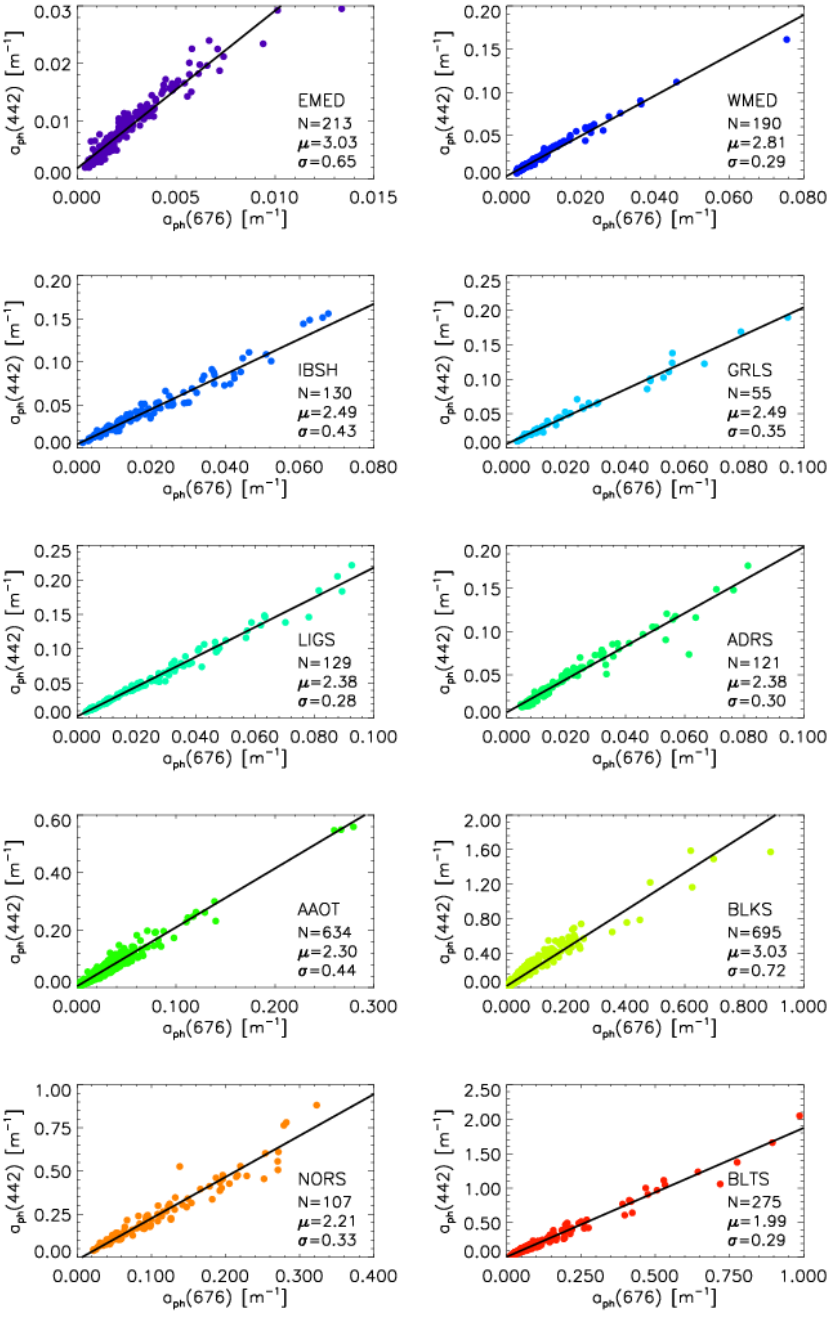

Figure 5. Scatter plots of $a_{ph}(442)$ versus $a_{ph}(676)$ in m^{-1} for the various geographic regions. N is the number of spectra, while μ and σ are the mean and standard deviation of the ratio $a_{ph}(442)/a_{ph}(676)$, respectively. Correlations coefficients (not shown) exhibit values within 0.96 and 0.99. The continuous thick black lines indicate the linear regression fits.

https://doi.org/10.5194/essd-2026-463
Preprint. Discussion started: 25 June 2026

5. Summary and conclusions

The CoASTS and BiOMaP measurement programs, established by the JRC Marine Optical Laboratory in collaboration with various European institutions, from 1995 up to 2022 produced a time-series and geographically distributed bio-optical data at the AAOT site in the northern Adriatic Sea and in European Seas, respectively. The measurements from the two programs included the same quantities rigorously obtained by applying standardized instruments, community measurement methods, extended quality control schemes and consolidated processing codes.

Complementary to a previous work that introduced the CoASTS-BiOMaP dataset comprising the near surface multispectral bio-optical data (see Zibordi and Berthon 2024), this work describes the CoASTS and BiOMaP dataset of hyperspectral absorption coefficients by pigmented and non-pigmented particles as well those by colored dissolved organic matter, both obtained applying spectrophotometric measurements to field samples. This unique dataset has relevance for bio-optical investigations supporting the exploitation of advanced hyperspectral satellite ocean color sensor data.

6. Author contributions

Jean-François Berthon and Giuseppe Zibordi equally contributed to the generation of the data set and to the writing of the manuscript.

7. Competing interests

Both authors declare no competing interest.

8. Data availability

Interested researchers can download the CoASTS-BiOMaP data set at https://doi.pangaea.de/10.1594/PANGAEA.993510 (Berthon and Zibordi 2026).

9. Acknowledgments

The authors acknowledge the contribution to field and laboratory activities by many JRC and international colleagues whose commitment made possible the execution of the multi-annual CoASTS and BiOMaP programs.

10. Funding support

Direct or indirect (through ship time) support to CoASTS and BiOMaP activities was provided by: the JRC through the EOSS and COLORS institutional projects, the European Union through the MAST-III, EUROFLEETS and JERICO programs, the North Atlantic Treaty Organization (NATO) through the Science for Peace Program, the US National Aeronautics and Space Administration (NASA), the European Space Agency (ESA), the Romanian Space Agency (ROSA), the Institute of Oceanology of the Bulgarian Academy of Sciences, the Institute of Oceanology of the Polish Academy of Sciences, the Finnish Environment Institute, the Italian National Research Council, the Portuguese Hydrographic Institute, the Italian Hydrographic Institute, the Royal Belgian Institute of Natural Sciences, the Hellenic Centre for Marine Research, the Université du Littoral Côte d' Opale.

https://doi.org/10.5194/essd-2026-463
Preprint. Discussion started: 25 June 2026

The contribution of Giuseppe Zibordi to the finalization of this work was supported by the National Aeronautics and Space Administration through the GESTAR-II program under award number 80NSSC22M0001, while the contribution of Jean-François Berthon was supported by DG DEFIS (the European Commission Directorate-General for Defence Industry and Space) and the Copernicus Programme.

11. References

Berthon, J. F., Mélin, F., and Zibordi, G.: Ocean colour remote sensing of the optically complex European seas. In *Remote sensing of the European seas* (pp. 35–52). Springer, Dordrecht, 2008.

Berthon, J.-F, Zibordi, G.: Coastal Atmosphere & Sea Time Series (CoASTS) and Bio-Optical mapping of Marine optical Properties (BiOMaP): the water hyperspectral absorption coefficients [dataset]. PANGAEA, https://doi.pangaea.de/10.1594/PANGAEA.993510, 2026.

Berthon, J-F., Zibordi, G., Doyle, J.P., Grossi, S., van der Linde, D. and Targa, C.: Coastal Atmosphere and Sea Time Series (CoASTS), Part 2: Data Analysis. *NASA Tech. Memo. 2002–206892, Vol. 20,* S.B. Hooker and E.R. Firestone, Eds., NASA Goddard Space Flight Center, Greenbelt, Maryland, 25 pp, 2002.

Ferrari, G. M., Dowell, M.D., Grossi, S., and Targa, C.: Relationship between the optical properties of chromophoric dissolved organic matter and total concentration of dissolved organic carbon in the southern Baltic Sea region. *Mar. Chem.*, 55(3–4), 299–316, 1996.

Ferrari, G. M., and Tassan, S.: A method using chemical oxidation to remove light absorption by phytoplankton pigments. *J. Phycology*, 35(5), 1090–1098, 1999.

IOCCG, 2000: Remote Sensing of Ocean Colour in Coastal, and Other Optically-Complex, Waters. Sathyendranath, S. (ed.), *Reports of the International Ocean-Colour Coordinating Group*, No. 3, IOCCG, Dartmouth, Canada.

Pérez, G.L., Galí, M., Royer, S.J., Sarmento, H., Gasol, J.M., Marrasé, C., and Simó, R.: Bio-optical characterization of offshore NW Mediterranean waters: CDOM contribution to the absorption budget and diffuse attenuation of downwelling irradiance. *Deep Sea Res. Part I Oceanogr.*, 114, 111–127, 2016.

Tassan, S., and Ferrari, G. M.: An alternative approach to absorption measurements of aquatic particles retained on filters. *Limnol. Oceanogr.*, 40(8), 1358–1368, 1995.

Tassan, S. and Ferrari, G.M.: A sensitivity analysis of the 'Transmittance–Reflectance'method for measuring light absorption by aquatic particles. *J Plankton Res*, 24(8), 757–774, 2002.

Tassan, S., Ferrari, G.M., Bricaud, A., and Babin, M.: Variability of the amplification factor of light absorption by filter-retained aquatic particles in the coastal environment. *J. Plankton Res.*, 22(4), 659–668, 2000.

Werdell, P.J., Cairns, B., Caplan, S.A., Cetinić, I., Foley, S.R., Franz, B.A., Gao, M., Fasnacht, Z.T., Huemmrich, K.F., Ibrahim, A. and Knobelspiesse, K.D.: Advancing Earth System Science With the NASA Plankton, Aerosol, Cloud, Ocean Ecosystem (PACE) Satellite Mission. *Glob. Chang. Biol.*, 32(4), doi.org/10.1111/gcb.70869, 2026.

Zibordi, G., and Berthon, J.-F.: Coastal Atmosphere & Sea Time Series (CoASTS) and the Bio-Optical mapping of Marine optical Properties (BiOMaP): the near-surface marine bio-optical data set. Accessible at: https://doi. pangaea.de/10.1594/PANGAEA.968716, 2024.

Zibordi, G., Berthon, J.-F., Doyle, J.P., Grossi, S., van der Linde, D., Targa, C. and Alberotanza, L.: Coastal Atmosphere and Sea Time Series (CoASTS), Part 1: A Tower-Based Long-Term

https://doi.org/10.5194/essd-2026-463
Preprint. Discussion started: 25 June 2026

590 Measurement Program. *NASA Tech. Memo. 2002–206892, Vol. 19,* S.B. Hooker and E.R.
591 Firestone, Eds., NASA Goddard Space Flight Center, Greenbelt, Maryland, 29 pp, 2002.
592 Zibordi, G., Berthon, J.-F., Mélin, F., and D'Alimonte, D.: Cross-site consistent in situ
593 measurements for satellite ocean color applications: The BiOMaP radiometric dataset. *Remote*
594 *Sens. Environ.*, 115(8), 2104–2115, 2011.
595 Zibordi, G. and Sciuto, P.: Advances in Marine Optics Technology, EUR 30996 EN,
596 Publications Office of the European Union, Luxembourg, ISBN 978-92-76-47719-8,
597 doi:10.2760/387681, JRC128393, 2022.
598

https://doi.org/10.5194/essd-2026-463
Preprint. Discussion started: 25 June 2026

Appendix A: Acronyms

AAOT	Acqua Alta Oceanographic Tower
ADRS	Adriatic Sea
BiOMaP	Bio-Optical mapping of Marine Properties
BLKS	Black Sea
BLTS	Baltic Sea
CDOM	Colored Dissolved Organic Matter
CoASTS	Coastal-Atmosphere and Sea Time-Series
EMED	Eastern Mediterranean Sea
GRLS	Greenland Sea
IBS	Iberian Shelf
LIGS	Ligurian Sea
MADP	Mean Absolute Percent Differences
JRC	Joint Research Center
NORS	North Sea
SPM	Suspended Particulate Matter
T-R	Transmission and Reflection spectrophotometric method
WMED	Western Mediterranean Sea